Porous-membrane second-sound transducers for superfluid ^{4}He

W. Zimmermann, Jr.
Tate Laboratory of Physics, University of Minnesota, Minneapolis, Minnesota 55455
(Received 1 July 1985)

A systematic analysis of porous-membrane second-sound transducers for superfluid ^{4}He is presented, based on the case of two transducers, one serving as generator, the other as detector, situated at opposite ends of a resonant cavity. Included in the analysis are the effects of viscous slip of the normal-fluid component in the pores of the membrane and the effects of the inertia of the fluid in the pores. The transducers are found to obey reciprocity relations connecting their efficiencies as generators and as detectors, for both first and second sound. The results are illustrated by numerical calculations for representative cases as functions of temperature and frequency.

I. INTRODUCTION

Vibrating porous-membrane second-sound transducers were introduced a number of years ago by Sherlock and Edwards[1] and by Williams *et al.*[2] and have been widely used since then. A number of recent articles have given valuable insight into the properties of such transducers.[3–11] These articles include both theoretical treatments and experimental studies. They have dealt with both the linear regime, in which the fluid flows remain subcritical, and, more lately, the nonlinear, supercritical regime.

The purpose of the present article is to give a somewhat more systematic development of the theory of the linear regime than has so far appeared. Although we use a number of simplifying assumptions similar to those used in the past, we allow for viscous slip of the normal-fluid component with respect to the membrane and we include the effects of the inertia of both fluid components flowing through the membrane. Thus we avoid the assumption that there is a vanishing chemical-potential difference between opposite faces of the membrane. As a result, our analysis should be applicable to membranes of any porosity, including the case of an impermeable membrane as a limit. In addition, our analysis should be applicable at higher frequencies than analyses which omit such inertial effects.

We show that, consistent with a reciprocity principle, the behavior of a transducer as a detector of first or second second is very closely related to its behavior as a generator of such sound. Our treatment is based on the case in which two transducers are coupled by a resonant cavity, and this coupling is treated explicitly. Our results are illustrated by representative numerical calculations. These calculations are compared where possible with those of Giordano, who has given a review of earlier work and presented a detailed analysis of transducer behavior in the linear regime.[7]

II. THEORY

A. Basic assumptions

Consider a cylindrical chamber with two porous-membrane diaphragms located near opposite ends, as shown in Fig. 1. Assume that the walls of the chamber are rigid and thermally insulating and that the chamber is completely filled with superfluid ^{4}He. Assume further that the membranes may undergo small pistonlike sinusoidal oscillations about their equilibrium positions. Let x_0 and x_5 denote the positions of the ends of the chamber and x_1 through x_4 the positions of fixed imaginary planes dividing the chamber into five parts, as shown in the figure.

We use the following linearized hydrodynamic equations, the only dissipative term included being the η_n term in the second equation:[12]

$$\rho_s \frac{\partial \mathbf{v}_s}{\partial t} \cong -\frac{\rho_s}{\rho}\nabla P + \rho_s s \nabla T \ , \tag{1}$$

$$\rho_n \frac{\partial \mathbf{v}_n}{\partial t} \cong -\frac{\rho_n}{\rho}\nabla P - \rho_s s \nabla T + \eta_n[\nabla^2 \mathbf{v}_n + \tfrac{1}{3}\nabla(\nabla\cdot\mathbf{v}_n)] \ , \tag{2}$$

$$\frac{\partial \rho}{\partial t} + \rho_s \nabla\cdot\mathbf{v}_s + \rho_n \nabla\cdot\mathbf{v}_n \cong 0 \ , \tag{3}$$

$$\frac{\partial}{\partial t}(\rho s) + \rho s \nabla\cdot\mathbf{v}_n \cong 0 \ . \tag{4}$$

Here, ρ_s, ρ_n, and ρ are, respectively, the superfluid, normal-fluid, and total densities, $\mathbf{v}_s$ and $\mathbf{v}_n$ the superfluid and normal-fluid velocities, P the pressure, T the temperature, s the entropy per unit mass, and η_n the normal-fluid viscosity. We will assume that the thermal-expansion coefficient of the fluid is zero.

In the arguments to come, we make frequent use of the

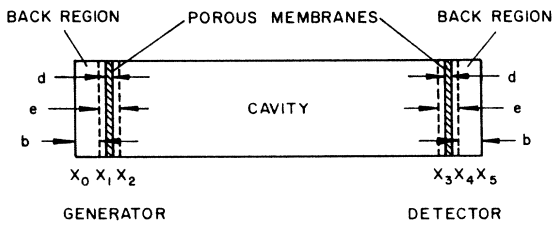

FIG. 1. Schematic drawing of the chamber with transducers and cavity.

following expressions for the velocities u_1 and u_2 of first and second sound:

$$u_1^2 \cong \frac{1}{\rho \kappa_s} , \tag{5}$$

$$u_2^2 \cong \frac{\rho_s}{\rho_n} \frac{s^2 T}{c_\rho} , \tag{6}$$

where κ_s is the (isentropic) compressibility and c_ρ is the heat capacity per unit mass (at constant density). In dealing with first and second sound it is convenient to work with the velocities

$$\mathbf{v} \equiv (\rho_s \mathbf{v}_s + \rho_n \mathbf{v}_n)/\rho , \tag{7}$$

$$\mathbf{w} \equiv \rho_s (\mathbf{v}_n - \mathbf{v}_s)/\rho , \tag{8}$$

instead of with $\mathbf{v}_s$ and $\mathbf{v}_n$, since for first sound $\mathbf{w} \cong 0$ and for second sound $\mathbf{v} \cong 0$.

Throughout, we will assume sinusoidal variation at a single angular frequency ω, with the time dependence of any variable A being given by the real part of $A_0 e^{-i\omega t}$, where A_0 is a complex amplitude. Except near (and within) the membranes, we will assume uniform conditions over any cross section of the chamber with velocities directed parallel to the chamber axis, the positive direction lying to the right.

B. Motion in the five regions

1. The back regions

We refer to the regions between x_0 and x_1 and between x_4 and x_5 in Fig. 1 as the back regions. Although the experimental back regions are typically the very thin (and often irregular) regions formed when the transducer membranes are stretched tightly over slightly uneven back plates, we will at the outset place no restriction on the thicknesses of these regions.

Consider the generator back region between x_0 and x_1. Let its thickness be b. Neglecting dissipation, we have for that region the wave equations

$$\frac{\partial^2 P}{\partial t^2} \cong u_1^2 \frac{\partial^2 P}{\partial x^2}, \quad \frac{\partial P}{\partial t} \cong -\rho u_1^2 \frac{\partial v}{\partial x} , \tag{9}$$

$$\frac{\partial^2 T}{\partial t^2} \cong u_2^2 \frac{\partial^2 T}{\partial x^2}, \quad \frac{\partial T}{\partial t} \cong -\frac{\rho_n}{\rho_s} \frac{u_2^2}{s} \frac{\partial w}{\partial x} . \tag{10}$$

Sinusoidal solutions to the first pair of equations represent first sound and take the form

$$P = P_0 e^{-i\omega t} = P_{+0} e^{i(k_1 x - \omega t)} + P_{-0} e^{i(-k_1 x - \omega t)} , \tag{11}$$

$$v = v_0 e^{-i\omega t} = v_{+0} e^{i(k_1 x - \omega t)} + v_{-0} e^{i(-k_1 x - \omega t)} , \tag{12}$$

where $k_1 = \omega/u_1$ and $P_{\pm 0} = \pm \rho u_1 v_{\pm 0}$. Setting $v_0 = 0$ at x_0, we find the following relation at x_1 between P_0 and v_0:

$$P_{10} = [\rho u_1 / i \tan(\omega b / u_1)] v_{10} . \tag{13}$$

Analogous solutions to the second pair of equations, with $k_2 = \omega/u_2$, represent second sound, and we find the following relation at x_1 between T_0 and w_0:

$$T_{10} = [\rho_n u_2 / i \rho_s s \tan(\omega b / u_2)] w_{10} . \tag{14}$$

Similar relations are obtained for the detector back region between x_4 and x_5.

2. The membrane regions

We refer to the regions between x_1 and x_2 and between x_3 and x_4 as the membrane regions. For the purpose of this development we assume that the membrane surfaces remain far enough away from the boundaries of the regions so that at these boundaries we may neglect the departures from uniformity in the fluid velocities at fixed x which occur near the membranes. At the same time we assume that the membrane regions are thin enough so that we may neglect any changes in the mass and entropy densities of the fluid in them and thus assume separately incompressible flows of the superfluid and normal-fluid components through these regions. In experiment, the scale of the irregularities in the back plates, the thicknesses of the back regions and of the membranes, and the distances between the pores of the membrane are typically of a similar magnitude. Thus the assumptions that we are making about the back and membrane regions, in order to make the analysis tractable, may not be accurately satisfied in practice.

In the following sections we consider the generator membrane region of thickness e with a membrane of thickness d.

a. Superfluid motion. Our assumption of incompressible superfluid flow in the membrane regions implies the assumption that $v_s(t)$ is the same at x_1 and x_2. Let $v_s(t)$ be given there by $v_{s0} e^{-i\omega t}$ and the membrane velocity $v_m(t)$ by $v_{m0} e^{-i\omega t}$. Under these conditions $\mathbf{v}_s(\mathbf{r},t)$ throughout the membrane region will be of the form $\mathbf{v}_{s0}(\mathbf{r}) e^{-i\omega t}$.

The amplitude $\mathbf{v}_{s0}(\mathbf{r})$ is governed by the differential equations

$$\nabla \cdot \mathbf{v}_{s0}(\mathbf{r}) = 0 , \tag{15}$$

$$\nabla \times \mathbf{v}_{s0}(\mathbf{r}) = 0 . \tag{16}$$

If we assume, in addition, that the superfluid circulations around all of the circuits threading the pores of the membrane are zero, these equations, together with the geometry of the region and the values of v_{s0} and v_{m0}, determine $\mathbf{v}_{s0}(\mathbf{r})$ uniquely. Because the differential equations satisfied by $\mathbf{v}_{s0}(\mathbf{r})$ are linear in $\mathbf{v}_{s0}(\mathbf{r})$ and because $\mathbf{v}_{s0}(\mathbf{r})$ is linearly dependent on the boundary-condition amplitudes v_{s0} and v_{m0}, we may write, by superposition,

$$\mathbf{v}_{s0}(\mathbf{r}) = \mathbf{a}_s(\mathbf{r}) v_{s0} - \mathbf{b}_s(\mathbf{r}) v_{m0} , \tag{17}$$

where $\mathbf{a}_s(\mathbf{r})$ and $\mathbf{b}_s(\mathbf{r})$ are unique dimensionless functions which are independent of v_{s0} and v_{m0}. Note that because membrane motion involves moving boundaries, our arguments here are only strictly valid to first order in v_{m0}.

However, $\mathbf{a}_s(\mathbf{r})$ and $\mathbf{b}_s(\mathbf{r})$ are not independent of each other. Consider the case in which $v_{m0} = v_{s0}$. In this case the superfluid in the membrane region will undergo solid-body oscillation with $\mathbf{v}_{s0}(\mathbf{r}) = \hat{\mathbf{x}} v_{m0} = \hat{\mathbf{x}} v_{s0}$, where $\hat{\mathbf{x}}$ is a unit vector in the x direction. Hence we have in general

$$\mathbf{a}_s(\mathbf{r})-\mathbf{b}_s(\mathbf{r})=\hat{\mathbf{x}}\ , \tag{18}$$

and we may write

$$\mathbf{v}_{s0}(\mathbf{r})=\hat{\mathbf{x}}v_{s0}+\mathbf{b}_s(\mathbf{r})(v_{s0}-v_{m0})\ . \tag{19}$$

Thus, $\mathbf{b}_s(\mathbf{r})$ describes the alteration in $\mathbf{v}_{s0}(\mathbf{r})$ due to the presence of the membrane.

We now integrate Eq. (1) from x_1 to x_2 along any path in the fluid. With some rearrangement we obtain

$$\frac{1}{\rho}(P_{20}-P_{10})-s(T_{20}-T_{10})=i\omega\int_1^2\mathbf{v}_{s0}(\mathbf{r})\cdot d\mathbf{r} \tag{20}$$

$$=i\omega e v_{s0}+i\omega d\gamma_s(v_{s0}-v_{m0})\ , \tag{21}$$

where γ_s is a dimensionless parameter defined as

$$\gamma_s\equiv\frac{1}{d}\int_1^2\mathbf{b}_s(\mathbf{r})\cdot d\mathbf{r}\ . \tag{22}$$

The parameter γ_s depends on the geometry of the membrane. For a totally porous membrane, we would have $\mathbf{b}_s(\mathbf{r})=0$ and $\gamma_s=0$. On the other hand, consider the case of a membrane with porosity (fractional open volume) α in the form of cylindrical channels with axes perpendicular to the membrane surface. An exact calculation of γ_s might be difficult for this case, particularly for channels of noncircular cross section. However, let us make the simplifying assumptions that plug flows occur in the channels and outside the membrane, and that the transitions between these flows which occur near the surfaces of the membrane (Saslow's "fuzzy" regions[5]) can be ignored. Then a brief argument yields

$$\gamma_s\cong(1/\alpha)-1\ , \tag{23}$$

which is always greater than zero.

Note that in Eq. (20) the left-hand side equals the difference $\mu_{20}-\mu_{10}$ in chemical potential per unit mass between x_2 and x_1. We see that this difference may be nonzero as a result of the inertia and acceleration of the superfluid in the membrane region. While in many practical situations this difference may be negligibly small, as has been assumed to some degree in most other analyses, our treatment allows for the possibility that this may not be the case, such as when α is made quite small or when ω becomes large, and includes the case of the impermeable diaphragm as the limiting case when $\alpha\to 0$.

b. Normal-fluid motion. Using parallel notation, we proceed for the normal fluid as we did for the superfluid. The differential equations governing the amplitude $\mathbf{v}_{n0}(\mathbf{r})$ are

$$\nabla\cdot\mathbf{v}_{n0}(\mathbf{r})=0\ , \tag{24}$$

$$-i\omega\nabla\times\mathbf{v}_{n0}(\mathbf{r})=(\eta_n/\rho_n)\nabla^2[\nabla\times\mathbf{v}_{n0}(\mathbf{r})]\ . \tag{25}$$

These follow from the incompressibility assumption and Eqs. (2) and (4). We assume that these equations, together with the boundary conditions, which include the specification of v_{m0} and of the magnitude v_{n0} of $\mathbf{v}_{n0}(\mathbf{r})$ at x_1 and x_2, determine a unique solution for $\mathbf{v}_{n0}(\mathbf{r})$.

The argument now proceeds in close analogy to that for the superfluid, and we obtain the equation

$$\mathbf{v}_{n0}(\mathbf{r})=\hat{\mathbf{x}}v_{n0}+\mathbf{b}_n(\mathbf{r})(v_{n0}-v_{m0})\ , \tag{26}$$

where $\mathbf{b}_n(\mathbf{r})$ is a unique dimensionless function. Integrating Eq. (2) along any path in the fluid from x_1 to x_2, we find

$$\frac{1}{\rho}(P_{20}-P_{10})+\frac{\rho_s}{\rho_n}s(T_{20}-T_{10})$$

$$=i\omega e v_{n0}+i\omega d\gamma_n(v_{n0}-v_{m0})\ , \tag{27}$$

where γ_n is a dimensionless parameter defined as

$$\gamma_n\equiv\frac{1}{d}\int_1^2\mathbf{b}_n(\mathbf{r})\cdot d\mathbf{r}+\frac{\eta_n}{i\omega d\rho_n}\int_1^2\nabla^2\mathbf{b}_n(\mathbf{r})\cdot d\mathbf{r}\ . \tag{28}$$

Like γ_s, γ_n will be difficult to determine precisely. For a totally porous membrane and zero fluid viscosity, we would have $\mathbf{b}_n(\mathbf{r})=0$ and $\gamma_n=0$. For a membrane with porosity α in the form of cylindrical channels with axes perpendicular to the membrane surface, we can consider two limits. With zero viscosity we would have an inertial contribution given by

$$\gamma_n\cong(1/\alpha)-1\ , \tag{29}$$

just as for the superfluid under similar approximations. On the other hand, if the viscous term in Eq. (28) dominates in the channels, and we have channels of circular cross section of radius a in which we may assume parabolic steady-state velocity profiles at each instant, and if we may ignore the transition regions near the membrane surfaces, a brief argument yields

$$\gamma_n\cong i\frac{8\eta_n}{\omega\rho_n a^2\alpha}=i\frac{4\delta_n^2}{a^2\alpha}\ , \tag{30}$$

where $\delta_n^2\equiv 2\eta_n/\omega\rho_n$ is the square of the normal-fluid viscous penetration depth. We will use the sum of Eqs. (29) and (30) as an approximate interpolation formula for γ_n.

c. Membrane motion. Let f be the net force per unit area exerted by the membrane on the fluid, and let $\mathscr{F}$ be the force per unit area exerted on the membrane by external means, such as an electric field. Assume, in addition, that the membrane is subject to an elastic restoring force per unit area $-k(x_m-x_{m,\mathrm{eq}})$, where k is the force constant per unit area and $x_{m,\mathrm{eq}}$ is the equilibrium value of the membrane position x_m. In practice, the membrane is supported by its edges and perhaps by random protrusions from the back plate, and the restoring force is provided by the membrane's elasticity. Our assumption of a pistonlike motion for the membrane with a Hooke's law restoring force is only a rough approximation to such a case.

With our assumptions, the equation of motion of the membrane is

$$\mathscr{F}-f-k(x_m-x_{m,\mathrm{eq}})=d\rho_m(1-\alpha)\dot{v}_m\ , \tag{31}$$

where ρ_m is the density of the solid material in the mem-

brane. Overall momentum balance for the fluid in the generating region (with separately incompressible components) gives us to first order

$$f-(P_2-P_1)=e\rho_s\dot{v}_s+e\rho_n\dot{v}_n-d\rho(1-\alpha)\dot{v}_m\ , \tag{32}$$

where v_s and v_n refer to the velocities at x_1 and x_2. Eliminating f between Eqs. (31) and (32), we obtain for sinusoidal motion

$$\mathcal{F}_0=P_{20}-P_{10}-i\omega e\rho_s v_{s0}-i\omega e\rho_n v_{n0}+i\omega d\rho\left[\frac{k}{\omega^2 d\rho}-r\right]v_{m0}\ , \tag{33}$$

where $r\equiv(1-\alpha)(\rho_m-\rho)/\rho$.

We may now collect the resulting equations for the generator membrane region and rewrite them in terms of v_0 and w_0, in place of v_{n0} and v_{s0}, as follows:

$$P_{20}-P_{10}=i\omega d\left[\left[\rho\frac{e}{d}+\rho_s\gamma_s+\rho_n\gamma_n\right]v_0+\rho_n(\gamma_n-\gamma_s)w_0-(\rho_s\gamma_s+\rho_n\gamma_n)v_{m0}\right]\ , \tag{34}$$

$$T_{20}-T_{10}=\frac{i\omega d}{\rho s}\left[\rho_n(\gamma_n-\gamma_s)v_0+\frac{\rho_n}{\rho_s}\left[\rho\frac{e}{d}+\rho_n\gamma_s+\rho_s\gamma_n\right]w_0-\rho_n(\gamma_n-\gamma_s)v_{m0}\right]\ , \tag{35}$$

$$-\mathcal{F}_0=i\omega d\left[-(\rho_s\gamma_s+\rho_n\gamma_n)v_0-\rho_n(\gamma_n-\gamma_s)w_0+\left[\rho_s\gamma_s+\rho_n\gamma_n-\frac{k}{\omega^2 d}+\rho r\right]v_{m0}\right]\ . \tag{36}$$

A similar set of equations applies to the detector membrane region, for which $\mathcal{F}_0$ would usually be zero.

3. *The cavity region*

If for the moment we neglect dissipation in the open cavity between x_2 and x_3, we have the same wave equations and the same general solutions for this region as we have for the back regions. Starting with Eqs. (11) and (12) for first sound, and letting

$$P_{20,\text{out}}\equiv P_{+0}e^{ik_1x_2},\quad P_{20,\text{in}}\equiv P_{-0}e^{-ik_1x_2}\ , \tag{37}$$

$$v_{20,\text{out}}\equiv v_{+0}e^{ik_1x_2},\quad v_{20,\text{in}}\equiv v_{-0}e^{-ik_1x_2}\ , \tag{38}$$

we have

$$P_{20}=P_{20,\text{out}}+P_{20,\text{in}}\ , \tag{39}$$

$$v_{20}=v_{20,\text{out}}+v_{20,\text{in}}\ , \tag{40}$$

$$P_{20}=\rho u_1(v_{20,\text{out}}-v_{20,\text{in}})\ . \tag{41}$$

Further, letting

$$P_{30,\text{in}}\equiv P_{+0}e^{ik_1x_3},\quad P_{30,\text{out}}\equiv P_{-0}e^{-ik_1x_3}\ , \tag{42}$$

$$v_{30,\text{in}}\equiv v_{+0}e^{ik_1x_3},\quad v_{30,\text{out}}\equiv v_{-0}e^{-ik_1x_3}\ , \tag{43}$$

we have

$$P_{30}=P_{30,\text{out}}+P_{30,\text{in}}\ , \tag{44}$$

$$v_{30}=v_{30,\text{out}}+v_{30,\text{in}}\ , \tag{45}$$

$$P_{30}=\rho u_1(v_{30,\text{in}}-v_{30,\text{out}})\ . \tag{46}$$

For second sound we have analogous relations. In particular, we have

$$T_{20}=T_{20,\text{out}}+T_{20,\text{in}}\ , \tag{47}$$

$$w_{20}=w_{20,\text{out}}+w_{20,\text{in}}\ , \tag{48}$$

$$T_{20}=\frac{\rho_n}{\rho_s}\frac{u_2}{s}(w_{20,\text{out}}-w_{20,\text{in}})\ , \tag{49}$$

$$T_{30}=T_{30,\text{out}}+T_{30,\text{in}}\ , \tag{50}$$

$$w_{30}=w_{30,\text{out}}+w_{30,\text{in}}\ , \tag{51}$$

$$T_{30}=\frac{\rho_n}{\rho_s}\frac{u_2}{s}(w_{30,\text{in}}-w_{30,\text{out}})\ . \tag{52}$$

So far we have ignored any dissipation in the cavity. However, in order to allow for such dissipation, as it might influence the width of a cavity resonance, let us make the following *ad hoc* modifications to our solutions in the cavity, ignoring any departures from uniformity over any cross section of the cavity. We replace k_1 wherever it appears above by $k_1+i\alpha_1$, where α_1 is a small attenuation coefficient for first sound, $\alpha_1\ll k_1$; and k_2 by $k_2+i\alpha_2$, where α_2 is a corresponding coefficient for second sound.

With these modifications, the local relationships at x_2 and x_3 given by Eqs. (39)—(41) and (44)—(52) are not upset. However, we obtain the following interconnections between x_2 and x_3:

$$v_{+0}=v_{20,\text{out}}e^{\alpha_1x_2}e^{-ik_1x_2}=v_{30,\text{in}}e^{\alpha_1x_3}e^{-ik_1x_3}\ , \tag{53}$$

$$v_{-0}=v_{20,\text{in}}e^{-\alpha_1x_2}e^{ik_1x_2}=v_{30,\text{out}}e^{-\alpha_1x_3}e^{ik_1x_3}\ , \tag{54}$$

$$w_{+0}=w_{20,\text{out}}e^{\alpha_2x_2}e^{-ik_2x_2}=w_{30,\text{in}}e^{\alpha_2x_3}e^{-ik_2x_3}\ , \tag{55}$$

$$w_{-0}=w_{20,\text{in}}e^{-\alpha_2x_2}e^{ik_2x_2}=w_{30,\text{out}}e^{-\alpha_2x_3}e^{ik_2x_3}\ . \tag{56}$$

C. Solution of the equations

The problem now before us is one of gathering together the linear algebraic equations for the various regions and

solving for the relationships between the amplitudes of interest. In particular, our goal is to determine the value of v_{m0} for the detector membrane for any given value of $\mathscr{F}_0$ applied to the generator membrane at any given value of ω, and to relate the amplitudes of the first and second sound transmitted by the cavity to these amplitudes. Because of the large number of variables and equations, we proceed in stages.

1. The generator: Reciprocity

We begin by eliminating P_{10} and T_{10} among Eqs. (13), (14), (34), (35), and (36). We then easily find

$$\frac{P_{20}}{i\omega d\rho}=\left[\frac{u_1}{i\omega d}\frac{1}{i\tan(\omega b/u_1)}+\frac{\rho_s\gamma_s+\rho_n\gamma_n}{\rho}+\frac{e}{d}\right]v_{20}+\frac{\rho_n}{\rho}(\gamma_n-\gamma_s)w_{20}-\frac{\rho_s\gamma_s+\rho_n\gamma_n}{\rho}v_{m0}\,, \tag{57}$$

$$\frac{sT_{20}}{i\omega d}=\frac{\rho_n}{\rho}(\gamma_n-\gamma_s)v_{20}+\frac{\rho_n}{\rho_s}\left[\frac{u_2}{i\omega d}\frac{1}{i\tan(\omega b/u_2)}+\frac{\rho_n\gamma_s+\rho_s\gamma_n}{\rho}+\frac{e}{d}\right]w_{20}-\frac{\rho_n}{\rho}(\gamma_n-\gamma_s)v_{m0}\,, \tag{58}$$

$$-\frac{\mathscr{F}_0}{i\omega d\rho}=-\frac{\rho_s\gamma_s+\rho_n\gamma_n}{\rho}v_{20}-\frac{\rho_n}{\rho}(\gamma_n-\gamma_s)w_{20}+\left[\frac{\rho_s\gamma_s+\rho_n\gamma_n}{\rho}-\frac{k}{\omega^2 d\rho}+r\right]v_{m0}\,. \tag{59}$$

In writing these equations we have arranged them so as to make evident the symmetry of the matrix of coefficients on the right-hand side. This symmetry, or that of the inverse matrix, gives rise to reciprocal relations of the type described by Rayleigh in which the terms on the left are regarded as "forces" and v_{20}, w_{20}, and v_{m0} as corresponding "displacements."[13]

However, for our purposes it is more suitable to eliminate P_{20}, T_{20}, v_{20}, and w_{20} and to introduce $v_{20,\text{in}}$, $v_{20,\text{out}}$, $w_{20,\text{in}}$, and $w_{20,\text{out}}$, using Eqs. (40), (41), (48), and (49). We then solve for "outputs" $v_{20,\text{out}}$, $w_{20,\text{out}}$, and v_{m0} in terms of the "inputs" $v_{20,\text{in}}$, $w_{20,\text{in}}$, and $\mathscr{F}_0$. This step involves lengthy but straightforward algebra. Nevertheless, it is possible to show without carrying out the full solution in detail that it has the form

$$(u_1/i\omega d)v_{20,\text{out}}=A_{vv}v_{20,\text{in}}+A_{vw}w_{20,\text{in}}+A_{vm}\mathscr{F}_0/2i\omega d\rho\,, \tag{60}$$

$$(\rho_n u_2/\rho_s i\omega d)w_{20,\text{out}}=A_{wv}v_{20,\text{in}}+A_{ww}w_{20,\text{in}}+A_{wm}\mathscr{F}_0/2i\omega d\rho\,, \tag{61}$$

$$v_{m0}=A_{mv}v_{20,\text{in}}+A_{mw}w_{20,\text{in}}+A_{mm}\mathscr{F}_0/2i\omega d\rho\,, \tag{62}$$

where the A coefficients form a symmetric matrix.

Hence with the proper (although nonunique) choice of variables [e.g., $(u_1/i\omega d)v_{20,\text{out}}$ in place of $v_{20,\text{out}}$] we have found for the generator a new set of reciprocal relations of an especially significant form. In particular, the equality of A_{vm} and A_{mv} means that the same coefficient governs the effectiveness of the "generator" as both a generator and detector of first sound, while the equality of A_{wm} and A_{mw} means the same for second sound.

For the purpose of further discussion emphasizing second sound, it is useful to rewrite the equations above in the following less symmetric form:

$$v_{20,\text{out}}=B_{vv}v_{20,\text{in}}+B_{vw}w_{20,\text{in}}+B_{vm}(\rho_s/2\rho\rho_n u_2)\mathscr{F}_0\,, \tag{63}$$

$$w_{20,\text{out}}=B_{wv}v_{20,\text{in}}+B_{ww}w_{20,\text{in}}+B_{wm}(\rho_s/2\rho\rho_n u_2)\mathscr{F}_0\,, \tag{64}$$

$$v_{m0}=B_{mv}v_{20,\text{in}}+B_{mw}w_{20,\text{in}}+B_{mm}(\rho_s/2\rho\rho_n u_2)\mathscr{F}_0\,. \tag{65}$$

The coefficients of primary interest to us are B_{vm}, B_{wm}, B_{mv}, and B_{mw}. Note that $B_{vm}=(\rho_n u_2/\rho_s u_1)A_{vm}$, $B_{mv}=A_{mv}$, $B_{wm}=A_{wm}$, and $B_{mw}=A_{mw}$, so that $B_{vm}=(\rho_n u_2/\rho_s u_1)B_{mv}$ and $B_{wm}=B_{mw}$. Hence once B_{mv} and B_{mw} are determined, B_{vm} and B_{wm} follow immediately, from these relations.

For B_{mv} and B_{mw} we find the following expressions:

$$B_{mv}=N_{mv}/D,\quad B_{mw}=N_{mw}/D\,, \tag{66}$$

where

$$N_{mv}=2i\frac{\rho_s\gamma_s+\rho_n\gamma_n}{\rho}\tan\beta_1(1-i\tan\beta_2)-2i\left[\gamma_s\gamma_n+\frac{e}{d}\frac{\rho_s\gamma_s+\rho_n\gamma_n}{\rho}\right]\delta_2\tan\beta_1\tan\beta_2\,, \tag{67}$$

$$N_{mw}=2i\frac{\rho_n}{\rho}(\gamma_n-\gamma_s)\tan\beta_2\left[1-i\tan\beta_1-\frac{e}{d}\delta_1\tan\beta_1\right], \tag{68}$$

$$D=\left[\frac{k}{\omega^2 d\rho}-r-\frac{\rho_s\gamma_s+\rho_n\gamma_n}{\rho}\right](1-i\tan\beta_1)(1-i\tan\beta_2)$$
$$+\left[-\left[\frac{\rho_s\gamma_s+\rho_n\gamma_n}{\rho}+\frac{e}{d}\right]\left[\frac{k}{\omega^2 d\rho}-r\right]+\frac{e}{d}\frac{\rho_s\gamma_s+\rho_n\gamma_n}{\rho}\right]\delta_1\tan\beta_1(1-i\tan\beta_2)$$
$$+\left[-\left[\frac{\rho_n\gamma_s+\rho_s\gamma_n}{\rho}+\frac{e}{d}\right]\left[\frac{k}{\omega^2 d\rho}-r\right]+\gamma_s\gamma_n+\frac{e}{d}\frac{\rho_s\gamma_s+\rho_n\gamma_n}{\rho}\right]\delta_2\tan\beta_2(1-i\tan\beta_1)$$
$$+\left[\left[\gamma_s\gamma_n+\frac{e}{d}(\gamma_s+\gamma_n)+\frac{e^2}{d^2}\right]\left[\frac{k}{\omega^2 d\rho}-r\right]-\frac{e}{d}\gamma_s\gamma_n-\frac{e^2}{d^2}\frac{\rho_s\gamma_s+\rho_n\gamma_n}{\rho}\right]\delta_1\delta_2\tan\beta_1\tan\beta_2\ . \tag{69}$$

Here we have introduced the dimensionless parameters $\beta_1\equiv\omega b/u_1$, $\beta_2\equiv\omega b/u_2$, $\delta_1\equiv\omega d/u_1$, and $\delta_2\equiv\omega d/u_2$.

The relative efficiency of first- and second-sound production by the generator can be measured by the ratio $v_{20,\text{out}}/w_{20,\text{out}}$ for a given $\mathcal{F}_0$ in the absence of $v_{20,\text{in}}$ and $w_{20,\text{in}}$. This ratio equals B_{vm}/B_{wm}. In agreement with Saslow[5] and others, we find that to a first approximation this ratio equals $\rho_n u_2^2/\rho_s u_1^2 \ll 1$ for some range of conditions, showing that such transducers are much more efficient generators of second sound than of first sound. However, in Sec. III we point out that significant deviations from this approximation can occur in practice.

The relative efficiency of first- and second-sound reception by the generator can be measured by the ratio of v_{m0} for a $v_{20,\text{in}}$ of a given magnitude, in the absence of $w_{20,\text{in}}$ and $\mathcal{F}_0$, to v_{m0} for a $w_{20,\text{in}}$ of the same magnitude, in the absence of $v_{20,\text{in}}$ and $\mathcal{F}_0$. This ratio equals

$$B_{mv}/B_{mw}=(\rho_s u_1/\rho_n u_2)B_{vm}/B_{wm}\ .$$

In agreement with Liu,[6] we thus find to a first approximation that this ratio equals $u_2/u_1 \ll 1$ for some range of conditions. Such transducers are thus also much less sensitive to first sound than to second sound when used as detectors, but the discrimination is not as great as it is for generation.

In their dependences on ω, both B_{mv} and B_{mw} are peaked at the resonance frequency of the transducer, due to the forms of their denominators D. The resonant mode can be thought of as an oscillation of the membrane, with inertial contributions from both the membrane itself and the accompanying fluid flow, under the influence of restoring forces provided both by the membrane elasticity and the pressure difference in the fluid. This resonance was recognized by Sherlock and Edwards,[1] who called it a Helmholtz resonance, but we believe that this name is somewhat misleading in view of the importance of membrane motion and inertia.[14] Care should be taken to note that their simple derivation of the resonance frequency is carried out in a low-temperature approximation. Further consideration of this resonance occurs in Sec. III. If b were to be made much larger than is usual, so that it could be of the same magnitude as the wavelength of first or second sound, then the transducer might possess more than one resonance.

In addition to B_{mv} and B_{mw}, we will need the coefficient of reflection for second sound B_{ww}. We obtain

$$B_{ww}=N_{ww}/D\ , \tag{70}$$

where

$$N_{ww}=-\left[\frac{k}{\omega^2 d\rho}-r-\frac{\rho_s\gamma_s+\rho_n\gamma_n}{\rho}\right](1-i\tan\beta_1)(1+i\tan\beta_2)$$
$$-\left[-\left[\frac{\rho_s\gamma_s+\rho_n\gamma_n}{\rho}+\frac{e}{d}\right]\left[\frac{k}{\omega^2 d\rho}-r\right]+\frac{e}{d}\frac{\rho_s\gamma_s+\rho_n\gamma_n}{\rho}\right]\delta_1\tan\beta_1(1+i\tan\beta_2)$$
$$-\left[-\left[\frac{\rho_n\gamma_s+\rho_s\gamma_n}{\rho}+\frac{e}{d}\right]\left[\frac{k}{\omega^2 d\rho}-r\right]+\gamma_s\gamma_n+\frac{e}{d}\frac{\rho_s\gamma_s+\rho_n\gamma_n}{\rho}\right]\delta_2\tan\beta_2(1-i\tan\beta_1)$$
$$-\left[\left[\gamma_s\gamma_n+\frac{e}{d}(\gamma_s+\gamma_n)+\frac{e^2}{d^2}\right]\left[\frac{k}{\omega^2 d\rho}-r\right]-\frac{e}{d}\gamma_s\gamma_n-\frac{e^2}{d^2}\frac{\rho_s\gamma_s+\rho_n\gamma_n}{\rho}\right]\delta_1\delta_2\tan\beta_1\tan\beta_2\ . \tag{71}$$

We find, as did Giordano,[7] that to a good approximation in many cases $B_{ww} \cong -1$, but we return to this point in Sec. III.

2. The detector

If we now derive equations for the detector analogous to Eqs. (63), (64), and (65) in terms of $v_{30,\text{in}}$, $v_{30,\text{out}}$, $w_{30,\text{in}}$, and $w_{30,\text{out}}$, we find that they are identical in form to Eqs. (63), (64), and (65) with subscript 2 replaced by subscript 3. Hence no further separate treatment of the detector need be carried out, and our remarks about detection by the generator apply equally well to the "detector."

3. Overall solution

A general solution for v_{m0} of the detector and for the sound-wave amplitudes in the cavity resulting from a given $\mathscr{F}_0$ applied to the generator is complicated because of the simultaneous presence of both first and second sound in the cavity. However, let us now use the fact that the transducers typically will be much better generators and detectors of second sound than of first sound. Further, let us restrict our attention to solutions near second-sound resonance peaks, which, except for accidental situations, will not coincide with first-sound resonances. Under these conditions, we will neglect first sound. The relevant equations for the generator and detector then become

$$w_{20,\text{out}} = B_{ww}(g) w_{20,\text{in}} + B_{wm}(g)(\rho_s/2\rho\rho_n u_2)\mathscr{F}_0(g) , \quad (72)$$

$$w_{30,\text{out}} = B_{ww}(d) w_{30,\text{in}} , \quad (73)$$

$$v_{m0}(d) = B_{mw}(d) w_{30,\text{in}} , \quad (74)$$

where the argument g denotes the generator and d the detector. When these equations are combined with Eqs. (55) and (56) for the cavity, we obtain

$$v_{m0}(d) = \frac{e^{i\kappa z}}{1 - B_{ww}(d)B_{ww}(g)e^{2i\kappa z}} B_{mw}(d)B_{wm}(g) \times \frac{\rho_s}{2\rho\rho_n u_2}\mathscr{F}_0(g) , \quad (75)$$

where $\kappa \equiv k_2 + i\alpha_2$ and $z \equiv x_3 - x_2$. The entire influence of the cavity is contained in the factor

$$C \equiv \frac{e^{i\kappa z}}{1 - B_{ww}(d)B_{ww}(g)e^{2i\kappa z}} , \quad (76)$$

which exhibits the cavity resonance peaks.

For the purpose of comparing Eq. (75) with experiment it is useful to note that for the case of narrow cavity resonances, a simple relationship exists between the maximum value of $|C|$ at a resonance peak $|C|_{\max}$ and the width of the peak $\Delta\omega$, defined as the interval between the values of ω at which $|C| = |C|_{\max}/\sqrt{2}$. For narrow resonances, for which we have $\alpha_2 z \ll 1$ and $|B_{ww}(d)B_{ww}(g)| \cong 1$ and the frequency dependence of $|C|$ over a peak is dominated by the frequency dependence of $e^{2ik_2 z}$ in the denominator, we find

$$|C|_{\max} \cong 1/[(1 - |B_{ww}(d)B_{ww}(g)|e^{-2\alpha_2 z})] \cong \frac{u_2}{z\Delta\omega} . \quad (77)$$

Here, $|C|_{\max}$ can also be expressed in terms of the quality factor of the resonance $Q = \omega_{\max}/\Delta\omega$, where $\omega_{\max}$ is the value of ω at which $|C| = |C|_{\max}$.

III. NUMERICAL EVALUATION

For illustration, we have evaluated our results numerically for representative experimental conditions. For comparison with Giordano's extensive calculations,[7] we chose the same set of Nuclepore filter membranes that he studied.[15] The properties of these are listed in Table I. We assumed the generator and detector to be identical in construction, with $b = 10$ μm, $e = 10$ μm, and $k = 566 \times 10^6$ N/m^3 corresponding to Giordano's $K = 100 \times 10^6$ g/s^2 for all the calculations, except as noted.

It should be remarked that with b comparable to d, the assumptions of the model are not well satisfied. The choice of e above represents a rather artificial compromise, since e should be larger than d by an amount sufficient to allow for transitional flow near the membrane surfaces, but small compared to b, insofar as the separate compressions of the fluid components play important roles in the back regions but are assumed not to occur in the membrane regions. However, we were reassured to find that an increase in e to 15 μm (or a decrease to 5 μm for the two thinner membranes) has a negligible effect on our results.

Thermodynamic data at saturated vapor pressure between 1.20 and 2.15 K were taken from the tables of Maynard,[16] supplemented at temperatures between 1.00 and 1.20 K by data from the work of Brooks and Donnelly,[17] adjusted to make smooth connections to Maynard's data. The values of the normal-fluid viscosity used were those given by Wilks,[18] interpolated with the aid of data given by Donnelly.[19]

We have carried out calculations up to a frequency of 100 kHz. For a second-sound velocity of 10 m/s, nearly the lowest value for which we have made calculations, the wavelength of second sound at this frequency is

TABLE I. Nuclepore filter membrane properties.

$\rho_m = 950$ kg/m^3 [a]			
Pore diameter d (μm)	Membrane thickness e (μm)	Areal density of pores (μm^{-2})	Porosity α
0.05	5[a]	6	0.012
0.10	5[a]	3	0.024
0.20	10	3	0.094
0.40	10	1	0.13
1.00	10	0.2	0.16
5.00	10	0.004	0.079

[a]We have used these values for uniformity with Giordano (Ref. 7). A recent catalog of the Nuclepore Corporation lists the bulk density of Nuclepore polycarbonate membrane material as 1200 kg/m^3 and the thicknesses of the 0.05- and 0.10-μm-diameter-pore polycarbonate membranes as 6 μm.

100 μm, still long compared to b, d, and e but perhaps just at the limit for the assumption of separate incompressibility to be valid in the membrane region.

A. Ratio of first-sound to second-sound generation and detection

Consider the ratios B_{vm}/B_{wm}, giving the ratio of v_0 to w_0 produced by the generator, and B_{mv}/B_{mw}, giving the relative amplitude sensitivity of the detector to first and second sound. We have compared calculated values of these ratios to their simple approximations given in Sec. II by calculating the quantity

$$R \equiv |B_{vm}/B_{wm}|/(\rho_n u_2^2/\rho_s u_1^2) = |B_{mv}/B_{mw}|/(u_2/u_1) \tag{78}$$

as a function of frequency from 0.1 to 100 kHz for all pore sizes at a representative sample of temperatures 1.1, 1.6, and 2.1 K. Figure 2 shows some representative plots of R versus frequency at 1.6 K.

For frequencies of 1 kHz and below, R was found to lie within the range from 0.97 to 1.12, showing the simple approximations to be relatively accurate there. As frequency increases, the approximations become less valid. At 10 kHz, R ranges from 0.3 to 5 and at 100 kHz, from 2 to 300.

B. Generation of second sound

The generation of second sound is governed by the coefficient B_{wm}, which equals $(2\rho\rho_n u_2/\rho_s)(w_{0,\text{out}}/\mathcal{F}_0)$ for $v_{0,\text{in}}=0$ and $w_{0,\text{in}}=0$. Figure 3 shows plots of $|B_{wm}|$ versus temperature at 4 kHz for all of our pore sizes.

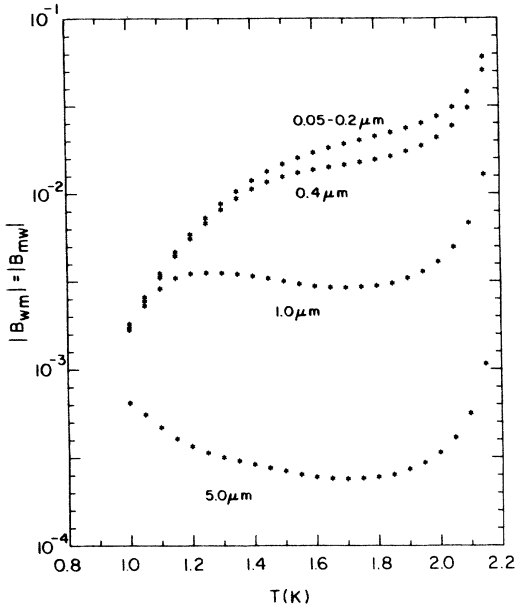

FIG. 3. Magnitudes of the second-sound generation and detection coefficients $|B_{wm}| = |B_{mw}|$ versus temperature for the various pore diameters at 4 kHz.

These results may be compared to Giordano's results for $|w_{\text{out}}/iF_0|$ shown in Fig. 9 of his work by computing $(\rho_s/2\rho\rho_n u_2)|B_{wm}|/A$, where $A=\pi(1.5)^2/4$ cm^2 is the area of his membrane.[7,20] The two sets of results are qualitatively very similar and at 1.0 K nearly coincide for all but the largest pore size. Otherwise, our values tend to lie below Giordano's by factors of up to 2.

It is important to keep in mind that B_{wm} is strongly frequency dependent. Figure 4 shows the variation of $|B_{wm}|$ at an intermediate temperature of 1.6 K for three

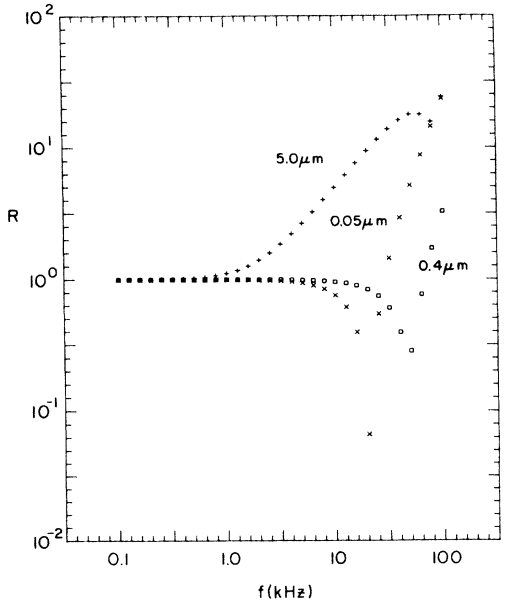

FIG. 2. Quantity R, which compares the relative efficiency for the generation or detection of first and second sound to a simple approximation for that quantity, versus frequency at 1.6 K for several pore diameters.

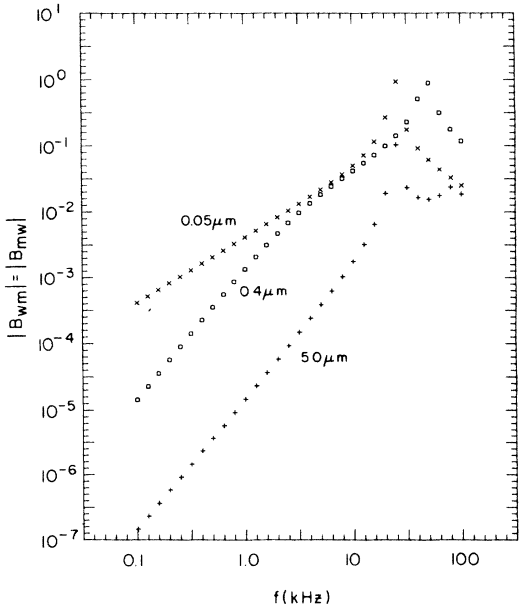

FIG. 4. Magnitudes of the second-sound generation and detection coefficients $|B_{wm}| = |B_{mw}|$ versus frequency for several pore diameters at 1.6 K.

representative pore sizes. At this temperature, in the interval from 0.1 to ~10 kHz, $|B_{wm}|$ ranges from varying as f for the smallest pores to varying as f^2 for the largest. The peaks which occur between 10 and 100 kHz reflect the transducer resonance. Similar behavior is seen at 1.1 and 2.1 K.

C. Detection of second sound

The detection of second sound is governed by the coefficient B_{mw}, which equals $v_{m0}/w_{0,\text{in}}$ when $\mathscr{F}_0=0$ and $v_{0,\text{in}}=0$. Because B_{mw} equals B_{wm}, the form of $|B_{mw}|$ also is illustrated in Figs. 3 and 4. Our results of Fig. 3 can be compared directly with Giordano's results for $|v_m/w_{\text{in}}|$ shown in Fig. 10 of his work.[7,20]

Our curves are qualitatively similar to Giordano's, except that for the 1.0-μm-diameter pores we find much less rise and fall. In general, our curves tend to lie above Giordano's. For pore sizes other than 1.0 μm, the discrepancy is no larger than a factor of 2 and is considerably smaller over much of the range. For 1.0-μm pores the discrepancy becomes as large as a factor of 8.

D. Overall response

Equation (75) relating $v_{m0}(d)$ to $\mathscr{F}_0(g)$ contains the product $B_{mw}(d)B_{wm}(g)$, which for identical generator and detector is just B_{wm}^2. We have compared our results for this quantity with Giordano's results for

$$|w_{\text{out}}/iF_0|\,|v_m/w_{\text{in}}|$$

shown in Fig. 11 of his paper by computing

$$(\rho_s/2\rho\rho_n u_2)\,|B_{wm}|^2/A\ .$$

The discrepancies noted earlier between our results and his for the generation and detection processes compensate each other to some extent. In summary we find that our values range from a factor of 3 smaller to a factor of 4 larger than Giordano's values.

It is particularly important here to note the strong frequency dependence of $|B_{wm}|^2$. Consistent with what we have said earlier about $|B_{wm}|$, at frequencies from 0.1 to ~10 kHz, $|B_{wm}|^2$ ranges from varying as f^2 for the smallest pores to varying as f^4 for the largest.

The ratio of $v_{m0}(d)$ to $\mathscr{F}_0(g)$ also depends on the cavity factor C. Note that C depends both on the transducers, through the product $B_{ww}(d)B_{ww}(g)$, and on the cavity itself, through the exponential e^{ikz}. We have evaluated the reflection coefficient B_{ww} between 1.00 and 2.15 K at 4 kHz for all of our pore sizes. We find that for the three smaller pore diameters, $|B_{ww}|$ drops below unity by at most 0.001 and for the three larger, by at most 0.011. The departures of $|B_{ww}|$ from unity tend to increase with frequency. At 4 kHz the phase of B_{ww} departs from π radians by a small amount which for all of our pore sizes increases with temperature, remaining less than 0.03 rad up to 2.00 K and increasing to 0.06 rad at 2.15 K.

E. Dependence on elastic constant

We have investigated the dependences of our numerical evaluations on the elastic constant k of the membrane. For comparison with corresponding results obtained from Giordano's Figs. 6, 7, and 8 for the generation and detection of second sound,[7,20] we chose a pore diameter of 0.4 μm, a frequency of 4 kHz, and values for k of 22.6×10^6, 113×10^6, and 566×10^6 N/m^3 to agree with his choices for K of 4×10^6, 20×10^6, and 100×10^6 g/s^2. Our results are qualitatively similar to Giordano's over the full range of temperatures studied by him, with discrepancies up to a factor of 2 in both directions. We also investigated the frequency dependence of these effects. A reduction of k enhances the generation and detection of second sound at 4 kHz and below by an amount which increases as the frequency is decreased and tends to lower the resonant frequency of the transducer. Note, however, that the ratio of first- to second-sound generation or detection is not influenced by k.

F. The inertia of the fluid in the pores of the membrane

We have investigated the influence of the inertia of the fluid in the pores of the membrane by performing calculations in which γ_s and the inertial part of γ_n were set artificially to zero. For reference, the values of these terms computed from Eqs. (23) and (29) and used for the main body of our calculations ranged from 5.3 to 82.3 for the various pore sizes. The length e was also set to zero in these calculations.

With the inertial terms set to zero, the normalized ratios R of first- to second-sound generation and detection amplitudes discussed above in Sec. III A are very close to unity at frequencies below 10 kHz. As the inertial terms are increased to the values computed from Eqs. (23) and (29), significant deviations of R from unity occur in both directions as discussed in Sec. III A and illustrated in Fig. 2. On the other hand, the values of $|B_{wm}|$ and $|B_{mw}|$ at 4 kHz are increased by at most a few percent by this increase. This finding supports the assumption made by other authors that for second-sound propagation, inertial effects in the membrane can be neglected, at least under some conditions. However, we see by implication that the inertial terms have a significant influence here on first-sound propagation.

At frequencies above 10 kHz, the influence of the inertial terms is much stronger. Although in the absence of the inertial terms R remains within 5% of unity up to 100 kHz at the temperatures sampled for all pore sizes, much larger deviations occur in R when the inertial terms are included, as illustrated in Fig. 2. In the absence of the inertial terms, the transducer resonance frequencies tend to be higher than with the inertial terms. As a result, the inclusion of the inertial terms increases $|B_{wm}|$ and $|B_{mw}|$ by amounts up to 65% at 10 kHz and decreases them by up to a factor of 70 at 100 kHz.

G. Viscous slip of the normal-fluid component in the pores of the membrane

The role of viscous slip of the normal-fluid component was investigated by performing calculations in which the normal-fluid viscosity was artificially increased at all temperatures and frequencies by a factor of 10^6, in order to

lock the normal-fluid motion to that of the membrane. At 4 kHz, $|B_{wm}|$ and $|B_{mw}|$ for the smaller pores were almost unchanged while for the larger pores they were increased, by as much as a factor of 100, so as to yield very nearly a single curve for the various pore sizes coincident with the uppermost curve in Fig. 3. A similar coalescence of values for different pore sizes was seen at other frequencies up to ~ 10 kHz. However, above 10 kHz, large differences between the various pore sizes remained. These observations support the proposal of Liu and Stern and the numerical results of Giordano that viscous slip can play an important role in the generation and detection of second sound by membranes with large pore diameters.[3,7]

IV. CONCLUSIONS

In this article we have presented a systematic treatment of porous-membrane transducers for (first and) second sound in the linear regime of behavior. Our treatment considers in particular the case of two transducers, one a generator, the other a detector, separated by a resonant cavity. In our analysis we have included the effects of viscous slip of the normal-fluid component in the pores of the membrane and the effects of the inertia of both the superfluid and normal-fluid components in the pores. These effects were expressed in terms of two parameters γ_s and γ_n using rather general fluid-dynamic arguments. The validity of our expressions given in terms of γ_s and γ_n should extend beyond the simple approximations used to estimate γ_s and γ_n.

The inclusion of viscous slip enables our results to extend to the case in which relatively large pores allow a significant amount of relative motion between the normal-fluid component and the membrane. The inclusion of inertial effects, which become increasingly important as the porosity of the membrane is decreased or the frequency raised, enables our results to extend to the limit of an impermeable membrane and to give a suitable account of transducer resonance under typical conditions. Our treatment gives a unified picture of a transducer as both a generator and a detector and provides useful reciprocity relations for both first and second sound.

We have illustrated our results and compared them to those of Giordano by means of numerical evaluations for Nuclepore filter membrane transducers. Although significant discrepancies exist, there is qualitative agreement between our calculations and his to a considerable extent. Our results support his finding that viscous slip of the normal-fluid component in the membranes with the larger pores plays an important role in reducing their efficiencies as transducers of second sound. In addition, we were surprised to find that the inertia of the superfluid component, even in membranes with porosities as low as 0.01, has very little effect at 4 kHz on the efficiencies of the transducers for the generation and detection of second sound, in further support of Giordano's work.

Our numerical evaluations show the strong frequency dependences of the efficiencies of the transducers as generators and detectors of second sound, including the peaks which occur at the transducer resonant frequencies. Inertial effects are seen to become important above 10 kHz and to play a strong role in determining the resonant frequencies.

Our results for $(\rho_s/2\rho\rho_n u_2)|B_{wm}|^2$ do not seem to provide a significantly better account of Giordano's experimental results than do his analytical results for the corresponding quantity, as judged by the temperature dependences of the curves for the various pore sizes. Our calculations for $k = 566\times 10^6$ N/m^3 give a reasonably good account of the temperature dependences for the four smaller pore sizes. However, the calculated temperature dependences for the two larger pore sizes are much greater than the experimental ones, rather independent of k. Thus we cannot yet say that accurate agreement has been established between theory and experiment.

ACKNOWLEDGMENTS

We gratefully acknowledge the support given this work by the Graduate School of the University of Minnesota and by the National Science Foundation.[21] We are indebted to N. Giordano, M. Liu, and F. Pobell for sending us copies of their work prior to publication and for discussion, and to D. Edwards and W. Saslow for correspondence.

[1]R. A. Sherlock and D. O. Edwards, Rev. Sci. Instrum. **41**, 1603 (1970).
[2]R. Williams, S. E. A. Beaver, J. C. Fraser, R. S. Kagiwada, and I. Rudnick, Phys. Lett. **29A**, 279 (1969).
[3]M. Liu and M. R. Stern, Phys. Rev. Lett. **48**, 1842 (1982).
[4]D. L. Johnson, Phys. Rev. Lett. **49**, 1361 (1982).
[5]W. M. Saslow, Phys. Rev. B **27**, 588 (1983).
[6]M. Liu, Phys. Rev. B **29**, 2833 (1984).
[7]N. Giordano, J. Low Temp. Phys. **55**, 495 (1984).
[8]N. Giordano, in *Proceedings of the 17th International Conference on Low Temperature Physics, Karlsruhe, 1984,* edited by U. Eckern, A. Schmid, W. Weber, and H. Wühl (North-Holland, Amsterdam, 1984), Part I, p. 307; J. Low Temp. Phys. **59**, 247 (1985).
[9]N. Giordano and P. Muzikar, in *Proceedings of the 17th International Conference on Low Temperature Physics, Karlsruhe, 1984,* edited by U. Eckern, A. Schmid, W. Weber, and H. Wühl (North-Holland, Amsterdam, 1984), Part I, p. 309.
[10]M. Grabinski and M. Liu, Phys. Rev. B **32**, 1856 (1985).
[11]G. Zimmermann and F. Pobell (unpublished).
[12]I. M. Khalatnikov, *Introduction to the Theory of Superfluidity* (Benjamin, New York, 1965).
[13]J. W. S. Rayleigh, *The Theory of Sound* (Dover, New York, 1945), Vol. I, Secs. 107–111.
[14]See, e.g., L. E. Kinsler and A. R. Frey, *Fundamentals of Acoustics,* 2nd ed. (Wiley, New York, 1962), Sec. 8.1.
[15]Nuclepore Corporation, Pleasanton, California.
[16]J. Maynard, Phys. Rev. B **14**, 3868 (1976).

[17]J. S. Brooks and R. J. Donnelly, J. Phys. Chem. Ref. Data **6**, 51 (1977).
[18]J. Wilks, *The Properties of Liquid and Solid Helium* (Oxford University Press, London, 1967), p. 669.
[19]R. J. Donnelly, *Experimental Superfluidity* (University of Chicago Press, Chicago, 1967), p. 234.
[20]The calculations presented in Figs. 6—11 of Ref. 7 were carried out for 4 kHz [N. Giordano (private communication)].
[21]Grant No. DMR-81-12973.